

We are IntechOpen, the world's leading publisher of Open Access books Built by scientists, for scientists

6,900

Open access books available

186,000

International authors and editors

200M

Downloads

Our authors are among the

154

Countries delivered to

TOP 1%

most cited scientists

12.2%

Contributors from top 500 universities



WEB OF SCIENCE™

Selection of our books indexed in the Book Citation Index
in Web of Science™ Core Collection (BKCI)

Interested in publishing with us?
Contact book.department@intechopen.com

Numbers displayed above are based on latest data collected.
For more information visit www.intechopen.com



X-Ray Scattering Techniques Applied in the Development of Drug Delivery Systems

Margareth Kazuyo Kobayashi Dias Franco,
Daniele Ribeiro de Araújo, Eneida de Paula,
Leide Cavalcanti and Fabiano Yokaichiya

Additional information is available at the end of the chapter

<http://dx.doi.org/10.5772/65326>

Abstract

The advances in nanotechnology have found application in different fields, such as food, agriculture, materials, chemistry, and medicine. However, one of the most important approaches is the development of nanocarriers and, in order to understand their structural organization, different physicochemical techniques have been used. In particular, small angle X-ray scattering (SAXS) and X-ray diffraction (XRD) have given important contribution to the study of organization phase of nanocarriers such as organic/inorganic nanoparticles, micelles, liposomes, cyclodextrins, polymers, and their interaction with drugs and other bioactive molecules. In this chapter, we will present theoretical aspects, experimental design, and the applications of both techniques for the development of delivery systems for bioactive molecules.

Keywords: drug delivery, diffraction, small angle X-ray scattering

1. Introduction

The term nanocarriers have been used to describe colloidal systems (emulsions, nanospheres, nanoparticles, nanocapsules, liposomes, and micelles) and other compounds such as natural, synthetic, organic, or inorganic materials (ceramic, bioglasses, organometallic compounds, carbon or peptide nanotubes etc.) with dimensions smaller than 500 nm for use as biomaterials, depots, implants, biosensors, vaccines, and biomarkers, in chromatography separation, diagnosis or imaging, and drug delivery systems (DDS) for bioactive

compounds such as peptides, proteins, oligonucleotides, nucleic acids, etc., as shown in **Figure 1**. Those carrier systems can be formulated into various preparations including suspensions, emulsions, capsules, tablets, gels, creams, and ointments for parenteral, oral, or topical use [1].

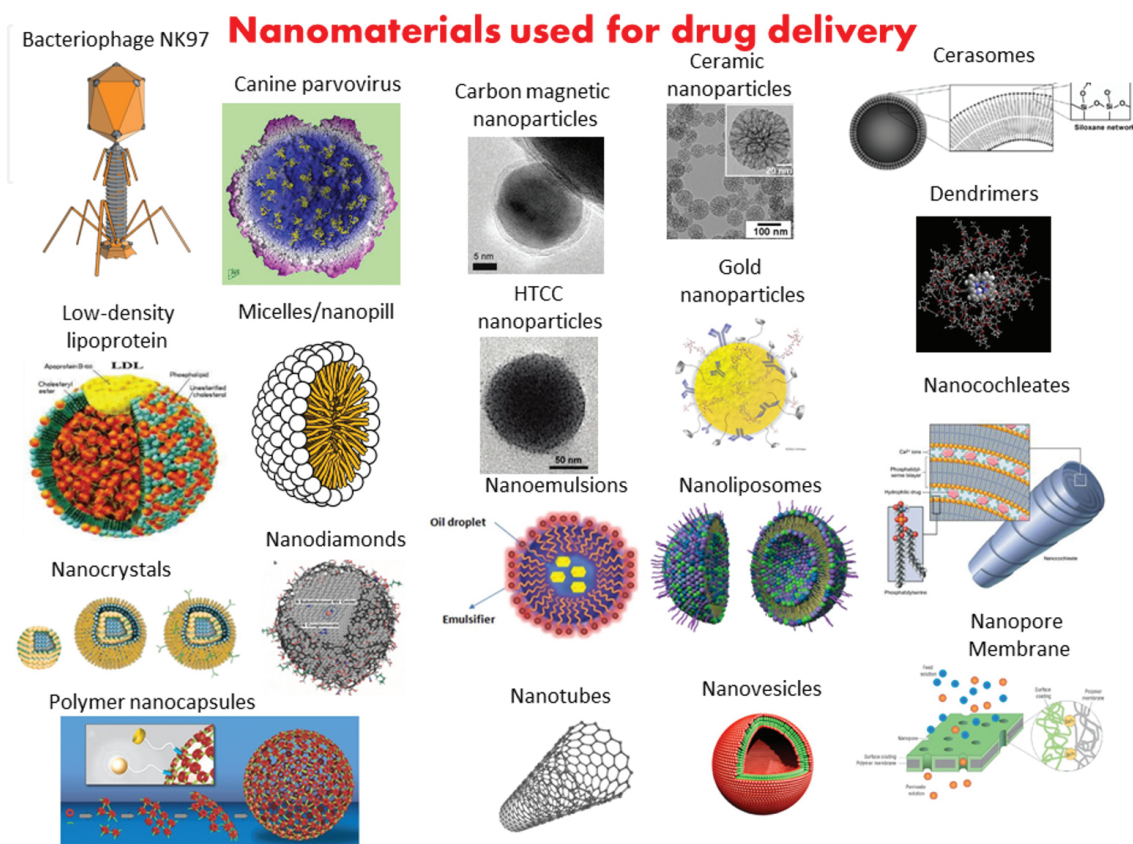


Figure 1. Examples of several drug delivery systems [2–20].

The development of new biomaterials, drug delivery systems (DDS), and modified release pharmaceutical formulations have allowed the modulation of physicochemical and biopharmaceutical properties of the several molecules, enhancing their therapeutic effects and promoting their clinical use. The different drug carriers described in the literature presented results specifically for molecules with limited aqueous or lipid solubility, low bioavailability, low stability, and high local or systemic toxicity [21].

The aim is the encapsulation of the bioactive molecule on a specific carrier destined to deliver it at a controlled rate over a prolonged period. The advantages of some DDS, such as nanoparticles, are their high circulation-residence time and drug bioavailability with enhanced therapeutic efficiency.

Despite several studies that report the physicochemical and biological applications of these nanocarriers, few studies have presented a relationship between their applications and structural aspects. In this chapter, our aim is to describe the basic concepts about X-ray scattering and its application for structural analysis of drug delivery systems.

This chapter explains the basic concepts of X-ray scattering and its applications in drug delivery systems. The basic equations for converting information obtained during the measurements in structural parameters of the object are also presented. We shall restrict ourselves to coherent and elastic small-angle X-ray scattering (SAXS), which is used in structural studies of soft condensed matter and in the X-ray diffraction (XRD) technique.

2. SAXS: small angle scattering technique

2.1. Introduction

Among drug delivery systems (DDS), carriers such as liposomes, micelles, hydrogels, and several kinds of hybrid organic-inorganic nanoparticles [22] can be found. For an effective or stable carrier, the colloidal size, which goes approximately from 1 nm to 1 μm , is an important criterion to select the delivery system that can permeate tissues, circulate with body fluids, or interact with cell membranes. Therefore, the structure is directly correlated with each function and the structural characterization of colloidal systems is in the range of the electron microscopy and X-ray scattering. In this study, we are going to discuss about small angle X-ray scattering (SAXS).

Unlike many other characterization techniques, the success of the SAXS study will highly depend on the prior knowledge available about the system. It means that one has to study thoroughly the sample preparation history, particle morphology, size distribution, aging stability, etc., before proposing SAXS method. The size distribution in the range of some hundreds of nm can be characterized by dynamic light scattering (DLS) [23] and the results can give a hint about agglomeration of the colloidal system that can favor polydispersity, which causes trouble in the resolution of the scattering signal in some cases. Mapping the aging stability is a crucial task in colloidal studies in order to have a fair referential for comparing a series of samples. Aging of colloidal systems can promote agglomeration or crystallization or even degradation and for each case, there will be a different scattering pattern. Morphology, studied using electron microscopy, prior to SAXS measurements, promotes an easier startup on the SAXS modeling and simulation. Fragile organic colloidal systems are better visualized through cryo-TEM (transmission electron microscopy) or cryofracture microscopy [24]. It is also important to know about the surface electric charges of the particles, through Zeta potential measurements [25], prior to SAXS measurements in order to facilitate the understanding of the interaction among all the sample constituents, which helps to build the most likely model structure to simulate the scattering intensity.

The SAXS technique is a nondestructive method and the experiment of scattering is relatively simple and fast. All the hard work will be charged on the treatment and analysis of the acquired data. Measurements taken for few days in a synchrotron lab will be enough for one whole year of analyzing data. Thus, the more you know about the system prior to the measurements, the more precise will be the experiment and the earlier you will be compensated by the information that can be determined through SAXS study.

2.2. Elements of SAXS theory

There are several good references for studying basic SAXS theory; the most popular is the book of Glatter and Kratky [26]. For amphiphilic systems, it is worth to check the article, also from Glatter, published in 1991 [27]; the work from Kratky on biological macromolecules, including some aspects from neutron scattering [28]; and more recent studies from our collaborators Trevisan et al. [29], showing the SAXS analysis for an example of modified liposomes after shearing preparation process, published in 2011; and the article of Oliveira et al. showing an efficient method to model and simulate SAXS intensity from unilamellar and multilamellar liposomes [30].

The SAXS technique comes from the fact that X-rays can interact with the electrons of the materials. When X-rays strike any matter, part of the energy is absorbed or transmitted. However, the part of the energy that is interesting for this technique is the one that scatters elastically (conserving the original frequency) depending on the structure of the material. The word “scattering” is already explaining everything about the method: instead of passing through the material, some photons are deviated (scattered) after the interaction with the electrons. The angle between the original direction of the photons and the deviation is called the scattering angle. The structure dimensions of the colloids are in the very size limits of the SAXS technique. The bigger the scattering objects, the smaller will be the scattering angle; this is the reason for calling this technique “small angle” scattering in contrast with the “wide angle” scattering used to study atomic distances.

The aim of the method is to study the scattering angle, or the scattering vector \vec{q} , in order to learn the characteristics of the object that caused the scattering. In this technique, the object is just a bunch of electrons with some structure. SAXS will give knowledge of the electronic density of the material and its spatial organization.

After X-rays strike the sample, the amplitude $A(\vec{q})$ of the scattered wave in the direction of the scattering vector \vec{q} is represented by the expression:

$$A(\vec{q}) = \rho(\vec{r})e^{-i\vec{q}\cdot\vec{r}} \quad (1)$$

where $\rho(\vec{r})$ is the average electronic density of the system and \vec{r} is the position of one atom of the material. The total amplitude scattered by all atoms of the material will be represented by the following expression:

$$F(\vec{q}) = \int \rho(\vec{r})e^{-i\vec{q}\cdot\vec{r}} d\vec{r} \quad (2)$$

which one can recognize as the Fourier transformation of the electronic density. The inverse Fourier transformation would yield the electronic density of the material, which is the very

subject of the study. But the SAXS experiment provides only the intensity of the scattered wave, which is the square modulus of the amplitude of the wave:

$$I(\vec{q}) = |F(\vec{q})|^2 \quad (3)$$

Extracting the electronic density of the material from the intensity $I(\vec{q})$ is not a straight forward task like the inverse Fourier transformation; it does not give a unique solution because we lost information of the phase of the wave when we squared the modulus; and that is why we need the support of the complementary techniques to find a reasonable model for the electronic density of the material.

On calculating the square modulus of the wave amplitude of Eq. (3), it could be understood that the expression of the intensity will be dependent not only on the electronic density of one point of the structure, but there will be a crossing term indicating that the intensity is the sum over the pair distance distribution function (PDDF) of the system, which expresses a contrast of the electronic density. This aspect is better explained with some examples of colloidal systems that naturally have this contrast of electronic density, for example, the contrast of electrons in proteins and the solution in which they are embedded; or liposomes and the buffer where they are dispersed; or even the contrast between the hydrogels and the pores that they form.

As the interaction with electrons is the origin of the phenomenon, the more electrons the materials have, the higher will be the intensity of the SAXS signal. Organic molecules have low electronic density compared to inorganic materials, so the signal is weak and the experiment need high brilliance sources like synchrotron facilities or lab equipment with enhanced optics for the best performance.

2.3. Experiment

The routine of the experiment is as follows:

Data acquirement: a sample is kept in front of the X-ray source and the scattering intensity at all angles is collected by a detector. Several facilities are prepared with special sample holders, environment conditions, *in situ* parallel techniques, and efficient detectors, as shown in **Figure 2**.

Data treatment: the scattering curve is recovered after data treatment which removes the background scattering caused by possible air gaps, windows, slits, or other parts of the instrumentation. Vacuum chambers are strategically placed to remove air gaps and light materials as beryllium, mica, and polymer films are used as windows to minimize spurious scattering.

Modeling: from the results of complementary techniques the parameters such as particle size, interaction among compounds, crystallization, polydispersity, etc., will help to build a model for the scattering object. For example, one can take a vesicle as a core of water surrounded by lipid bilayers and this model is known as core-shell structure. The size of the core and shell,

as well as the shape of objects interacting with this core-shell phase or the particles that can exist dissolved or crystallized in water, will all be a part of the model. There are several known models to start the approach of the scattering object, for instance, hard or hollow spheres, cylinders or other shapes, and also combined models for polydispersed systems. The scattering of these objects are called form factor scattering in contrast with structure factor, which is related to the periodicity of the shapes that can exist in some systems, for example, in multi-layered liposomes.

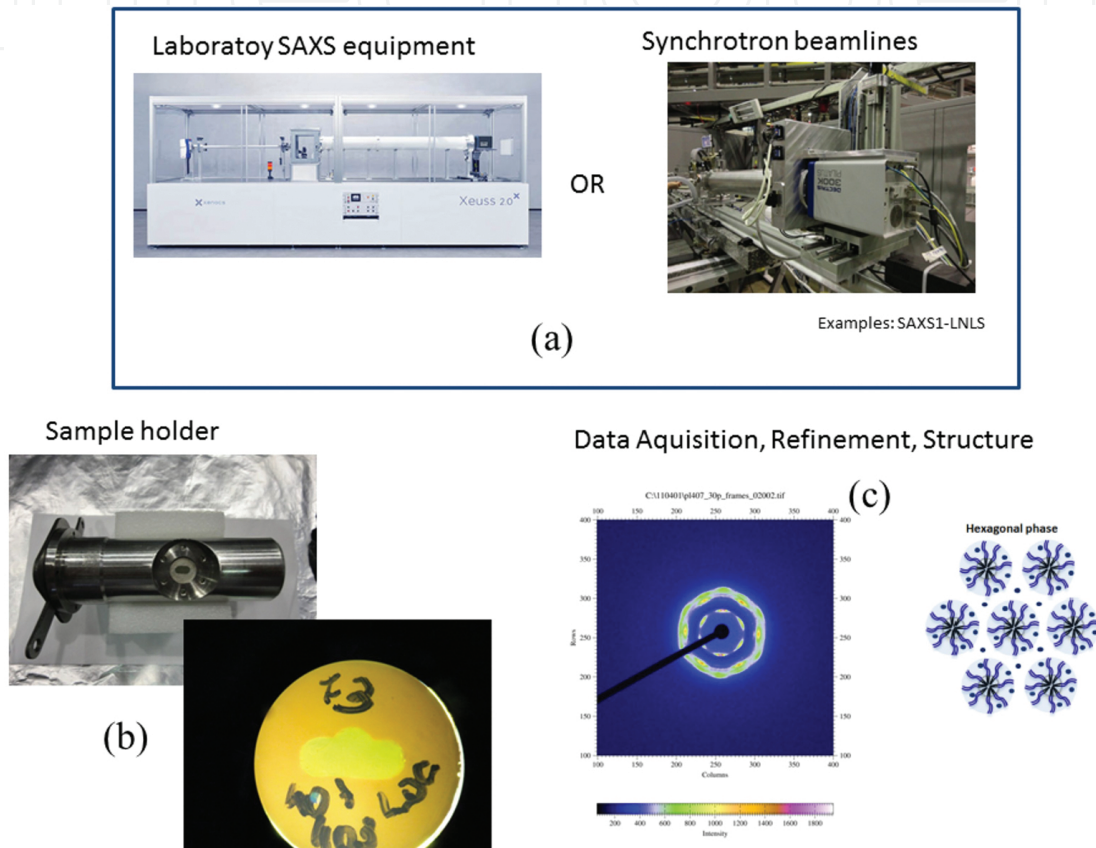


Figure 2. (a) Laboratory SAXS equipment or Synchrotron SAXS beamline can be used to characterize drug delivery systems. (b) Sample holder pictures; (c) some results from poloxamer systems used as drug delivery systems obtained using the SAXS technique [31].

Simulation: after having a model one can calculate the scattering intensity of the model, which is easier if done by computing programs. There are several software tools on the market for SAXS analysis that offer ready-to-use form factors like the ones that we commented before: hard spheres, core-shell, etc. Some software tools even offer possibilities to build your own form factor, considering more complex models.

Fitting: the final step is to compare the simulated scattering intensity with the experimental data. If they fit together, this is the end of the process and one can assume that the chosen model is a reasonable structure supported by all experimental results, not only SAXS, but everything else that helped to build the model. If the simulation does not fit the experimental

data, one can make adjustments on the model, make another simulation and compare again until it fits as good as they want.

In the study of Brzustowicz and Brunger [32], they used a model of hard spheres to fit the dispersion of stearyloleoyl phosphatidylserine (SOPS) micelles in buffer. This study used a monodisperse micelle sample with the main purpose to propose a different approach for analyzing lipid bilayer SAXS data. The graph of **Figure 3** of that paper shows a perfect fitting between calculated and experimental data. The results were good to determine the size of the inner core of the liposome and the electronic density profile across the membrane.

A successful SAXS analysis was reported in the work of some collaborators Gasperini et al. [33] after Balbino et al. [34]. In both cases, a biopolymer was inserted in liposome dispersions, hyaluronic acid (HA), and DNA, respectively. The results indicate that there are similarities at low concentration of incorporation of polymer inside the liposome dispersion. The negatively charged polymers bonded together neighbor unilamellar cationic liposomes like an electrostatic plastic glue. At higher concentrations of polymer, one can observe distinct behavior for these two biopolymers: DNA succeeded to disrupt the lipid membrane promoting the organization of multilamellar liposomes; and HA was able to coat individual unilamellar liposomes stabilizing the dispersion.

The SAXS analysis of these two studies, together with the results of the complementary techniques, was able to reveal all these details. For this, the liposome preparation was carefully controlled to have minimum polydispersity and the systems were studied strictly under the aging stability period. Several methods were used as complementary techniques such as DLS, zeta potential, TEM, cryo-TEM, and chromatography to help build the structure model to calculate the simulated scattering to be compared to the SAXS experimental data. Reasoning aspects were considered to minimize fitting parameters to increase the reliability of the results.

For other nanocarriers, such as thermosensitive poloxamer (or Pluronic® -PL)-based micelles and hydrogels (see **Figure 3**), SAXS technique have presented important contributions for understanding the structural changes after the incorporation of drugs/carriers or the formation of systems composed of PL with different hydrophilic-lipophilic balance (HLB).

SAXS studies have reported the formation of wormlike micelles for PL-P84 [35]; the gelation mechanisms and micelle packing under hexagonal and body-centered cubic phases for PL-P85 and PL-F88, respectively. However, for the PL-F88/PL-P85 mixture, the destabilization of the hexagonal phase after PL-F88 addition [36], a PL with higher HLB (28) compared to PL-P85 (16) was observed [37]. Other authors also reported SAXS analysis for PL-based binary hydrogels (PL concentrations ranging from 20 to 30% m/v) with different HLB values, such as PL-F127/PL-F68 [38] and PL-F127/PL-L81 [39], being observed in the formation of a hexagonal phase at physiological temperature and their purpose as sumatriptan and ropivacaine delivery systems for application by infiltrative routes. However, for fluid systems (with PL concentrations lower than 18% m/v) the binary micelles composed of PL-F127/PL-L81 presented a lamellar phase structural organization, even after the incorporation of the drug chlorpromazine [40].

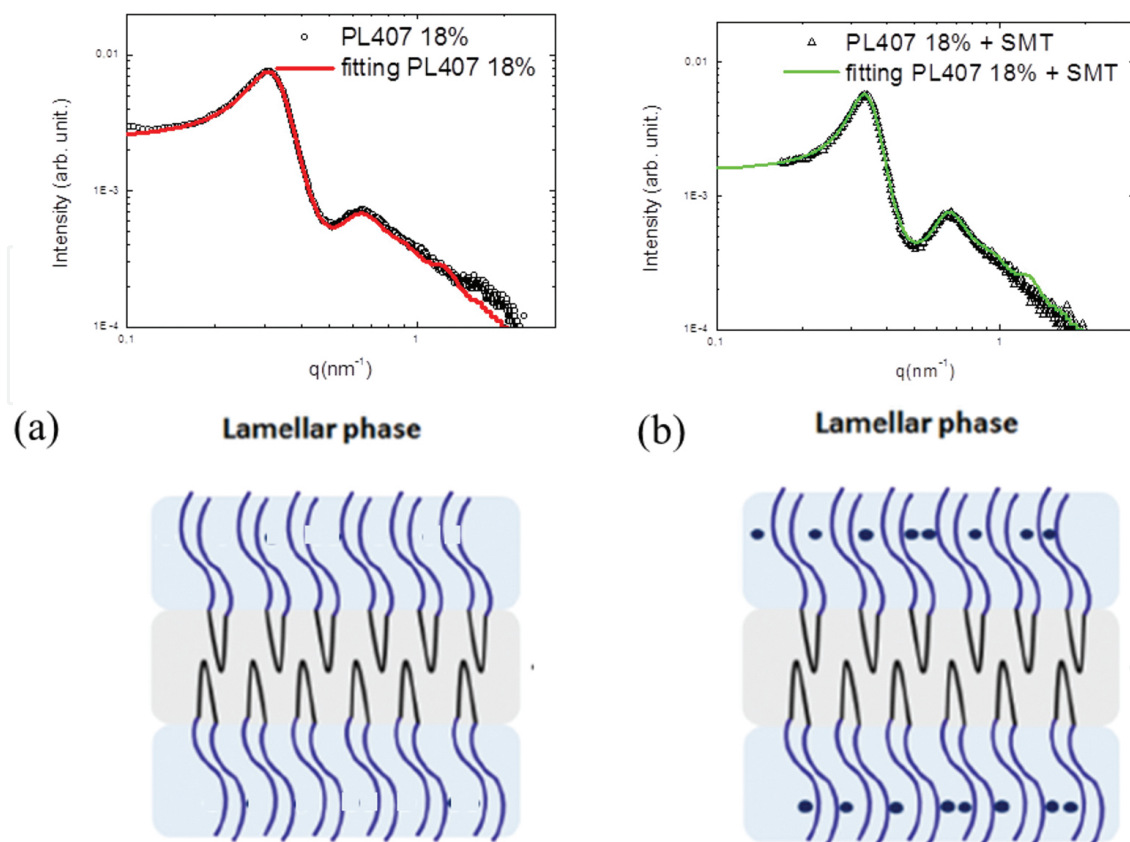


Figure 3. Example of successful SAXS analysis of a drug delivery system based on poloxamers (a) poloxamer without drug; (b) poloxamer with sumatriptane (SMT).

In fact, the drug incorporation of PL-based systems, studied by SAXS, has been highlighted in the literature. In a recent work, Avachat and Parpani [41] described the formulation of liquid crystal nanoparticles for efavirenz oral delivery. The study showed the formation of cubosomes after the incorporation of PL-F127 and phytantriol, a cosmetic ingredient. Chen et al. [42] studied the acetaminophen and bifonazole crystallization mechanism within polyethylene glycol (PEG), polypropylene glycol (PPG), and PL-F127 matrices, observing an improvement of crystallization rate for both drugs.

Another innovative approach relates to the combination of different carrier systems (natural and synthetic, for example) that perform different functions, usually synergistic, in the same pharmaceutical formulation. These new carriers, hybrid systems, can provide (in combination) levels of structural organization and different biopharmaceutical properties of the individual carriers, being used as a strategy to overcome limitations in relation to the physicochemical properties (such as aqueous solubility), pharmacokinetic (control local absorption and/or uptake to the bloodstream), pharmacodynamic (increased drug duration of action) or toxicological properties (improvement in biocompatibility, reduced local and systemic toxicity) [43, 44]. In this sense, the interactions and the structural patterns formed between PL and cyclodextrins, inorganic nanoparticles, and natural or synthetic polymers have been described in the literature.

SAXS studies revealed a face-centered cubic phase for PL-F127 hydrogels (30 wt%) after interaction with PEG 6000 or PEG 35000 and polyvinylpyrrolidone [45]. On the other hand, the PL supramolecular structure was destabilized after incorporation of Fe₃O₄ nanoparticles into PL-F108 hydrogels, showing that the thermogelation is due to the clustering of nanoparticles into a fractal network [46]. In a different manner, a cubic symmetry was observed by SAXS characterization of the systems composed of ordered mesoporous silica nanoparticles in PL-F127 hydrogels [47].

For other nanocarriers, such as cyclodextrins (CD), different structural arrangements have been described, being also related to the delivery capability of those systems. Simões et al. [48] reported the development of a syringeable hydrogel composed of PL-F127 and α -CD for the delivery of vancomycin. In others reports, the incorporation of α -CD, studied by SAXS, showed a significant change on gelation behavior of PL-F68 and PL-F127 due to the formation of polypseudorotaxane (interaction of the hydrophobic PL unimers with the hydrophobic cavity of CDs, stabilized by noncovalent bonds, van der Waals forces, and interactions between the hydroxyl groups of adjacent CDs and hydrophilic polyethylene glycol polymer unimers) supramolecular complexes, in a similar manner observed in the interaction between β -CD and PL-F108 [49, 50].

3. X-ray diffraction

3.1. Introduction

One of the biggest challenges of the pharmaceutical science is to understand how the drugs interact with the cells in the body. This study is directly linked to physical and chemical properties of the drugs and the drug delivery systems. Therefore, it is important and necessary to use appropriate techniques for characterization, suitable for the development and improvement of the efficacy of the drugs.

For this reason, X-ray diffraction techniques stands out amongst several characterization techniques to distinguish the solid forms, like salt, polymorphs, solvates and cocrystal, and amorphous forms. X-ray diffraction provides information about the long ordering crystalline samples and also short ordering in vitreous or amorphous materials. This technique helps to relate the X-ray diffraction patterns with the structural ordering or disordering in materials science. It is worth to note that there is a clear difference between the crystalline materials, and amorphous and vitreous materials when observed via X-ray diffractometer. In the X-ray diffraction pattern for crystalline materials, several sharp peaks can be observed. On the other hand, for vitreous or amorphous materials the diffraction pattern display typically three or less halos (large peaks).

In 1999, Wunderlich [51] proposed a classification system based on the structural ordering and molecular packing present in the organic forms using three ordering parameters: translation, orientation, and conformation, as summarized in **Table 1**.

Solid form	Translation	Conformation	Orientation
Crystal	Long order	Long order	Long order
Condis Crystal	Long order	Short order	Long order
Plastic Crystal	Long order	Short order	Short order
Liquid Crystal	Short order	Short order	Long order
Vitreous or amorphous	Short order	Short order	Short order

Table 1. Classification system of solid forms as described by Wunderlich [51].

Solid-form crystals with a long ordering structure can be indexed characterized using X-ray powder diffraction technique (XRPD) due to its unique combination of order parameters. Although the solid forms of amorphous and vitreous materials do not exhibit any long ordering structure, they can be identified and characterized by their local molecular (short) ordering.

Some applications of X-ray diffraction techniques used to analyze the properties of the solid state of the drugs are: (1) characterizing the ordering in the active pharmacological ingredient (API); (2) identifying the existence forms in the API; (3) determining the solid form of API in the final drug product; (4) determining the physical and chemical stabilities; (5) identifying the components existing in the drug product; (6) detecting impurities or contaminants in the drug product; (7) monitoring changes in the sold form of the drug due to the fabrication; and (8) analyzing quantitatively and qualitatively the final drug product.

Based on the sensitivity of the technique to the ordering of structure, with appropriate data obtained from XRPD, it is possible to determine the structure of the solid forms and also the packing of the molecules in the solid. This information contributes significantly in the understanding of the chemical content in the solid state of the drug. Moreover, it is also important from the regulatory perspective.

3.2. Elements of diffraction theory

The X-ray diffraction technique measures the X-ray photons after the collision with the electronic cloud of the sample that changes the photon trajectory, though keeping the same phase and energy of the incoming photon. This is the key concept of the coherent elastic scattering process.

In organic samples, there are some specific facts that must be considered:

1. The application of a mathematical simplification known as first Born approximation is important and useful in the explanation of the X-ray diffraction process.
2. As expected, the interaction of the solid forms in the organic samples with incoming X-ray beam is weak and the amplitude of the multiple radiation scattering is almost negligible when compared to the simple radiation scattering.

3. In the presence of crystal defects, grain boundary or disordering systems, the multiple radiation scattering become even less significant.

Based on these considerations and their limits, we can model the process of diffraction as a Fourier transform of the electronic density inside the sample.

While each atom is considered a specific source of scattering process, the molecules can also be reduced to specific sources of scattering, considering that the distribution of the electronic density of a collective set of atoms is the sum of electronic density distribution attributed to centralized atoms individually.

Although the atoms in a molecule are not necessary the same as the free atoms, they are frequently considered as being free atoms. In this way, the ordering of the specific centers of scattering in the real space produces a group of diffraction events in the reciprocal space that corresponds to the intensity of the peaks.

A d spacing between the punctual centers (molecules) in the real space corresponds to a peak of the $\frac{2\pi}{d}$ spacing in the reciprocal space (also called Q -space).

As the Fourier transform can be applied in any molecular translational ordering that exists inside a solid form, the diffracted peak positions can be expressed in terms of d -space, Q -space or, more common, in 2θ .

In order to cause a constructive interference of the scattered waves, it is necessary that the Bragg's law be obeyed. The Bragg's law relates the X-ray scattering angle θ with the d -spacing parameter, as shown in **Figure 4**.

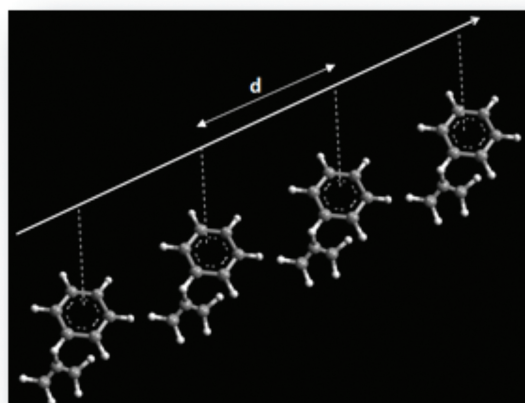


Figure 4. Representation of a simple periodic array of an organic molecule with a single orientation and conformation. The molecules are periodic, separated by a constant spacing d .

$$n\lambda = 2d \sin \theta \quad (4)$$

where λ is wavelength of the incident radiation; n is an integer number; d is interplanar distance to a set of hkl planes of the crystalline structure; θ is X-ray incident angle, as shown in **Figure 5**.

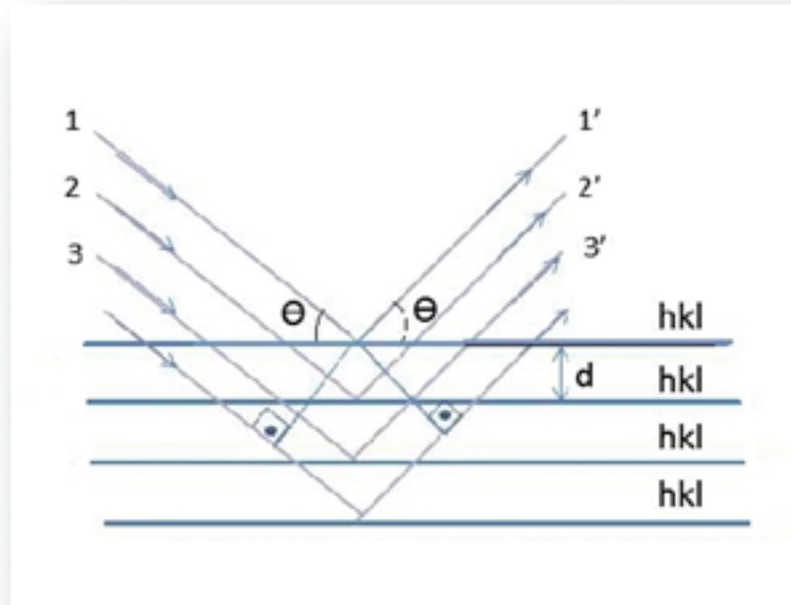


Figure 5. Schematic representation of the Bragg's law for the X-ray diffraction.

The samples analyzed by the X-ray diffraction technique can be in the powder form or solid with plane surfaces.

Analyzing the diffractogram of a polycrystalline sample, we verify that the peaks related to different set of planes show different intensities. If we build a diffractogram using just geometric aspects (Bragg's law), we will expect that all the peaks display the same intensity since all of them are subjected to constructive interference.

However, there are several physical aspects that influence the intensity of the peaks in a diffractogram, such as:

- Atomic scattering factor (this value indicates how an atom can scatter to a certain angle in a certain wavelength).
- Structure factor (quotient of amplitudes of scattered waves by all the atoms in a unit cell and the amplitude of the scattered wave by one electron).
- Multiplicity factor (there are planes that, for having the same interplanar distance, scatter to the same peak. This is the case, for instance, of 100, 010, and 001 planes in a cubic cell. Adding also the planes, with -1 instead of 1 , we have in total six planes contributing to the same peak, implying in a factor of multiplicity 6).

In order to get the expression for the intensity, we need three more correction factors: (a) Lorentz factor, (b) polarization factor, and (c) temperature factor. The first two are related to the geometric corrections that affect the diffracted intensity. Finally, the last one is related to temperature process that can cause shift in the position of the peaks, decreasing the intensity of the peaks and increasing the background.

A more complete explanation of the expression for the intensity and the factor that affects the intensity can be found in the reference of this chapter [52–57].

3.3. Experiment

The optics and the instrumentation used in the X-ray diffraction technique are directly related to the type of the X-ray source. However, we can define three generic elements: X-ray source, sample (including here the sample holder and sample environment, such as furnaces and cryostat), and detector.

An optimized experiment has as premise the following three conditions:

- Suitable X-ray source with efficient beam conditioning.
- A sample properly prepared, an optimized sample holder with low background and minimum influence in the measurement, and an appropriated sample environment that allows a stabilization of the sample in certain conditions as for example, temperature.
- Optimized detection systems (with or without optics to reduce background and to focus the scattered beam in order to improve the signal to noise ratio).

3.3.1. Experimental procedures of X-ray diffraction

The diffractograms show the diffracted intensities as a function of experimental parameter 2θ (angle between the diffracted and undeviated X-ray waves). The intensity is typically expressed in counts or counts per seconds while the peaks are listed as positions in degrees or in d -spacing (measured in Å or nm).

3.4. Crystalline materials

For materials with long ordering structure (crystalline materials) the diffractograms show sharp peaks, which the shape and the width depend on the instrument geometry where the data were collected. In **Figure 6**, we display an example of a diffractogram of a drug delivery system, β -cyclodextrin. The measurements were performed in a conventional diffractometer with Cu radiation, and, it was possible to perform a Rietveld refinement to obtain the final structure (as shown in the insert of **Figure 6**).

The range of the measurement for crystalline materials depends on the aim of the study. For example, when we study big molecules (for instance, biological samples), it is beneficial to measure at low angles, allowed by the geometry of the instrument (approximately 0.5° can be reached in a typical laboratory configuration in modern instruments or less than 0.5° using synchrotron sources).

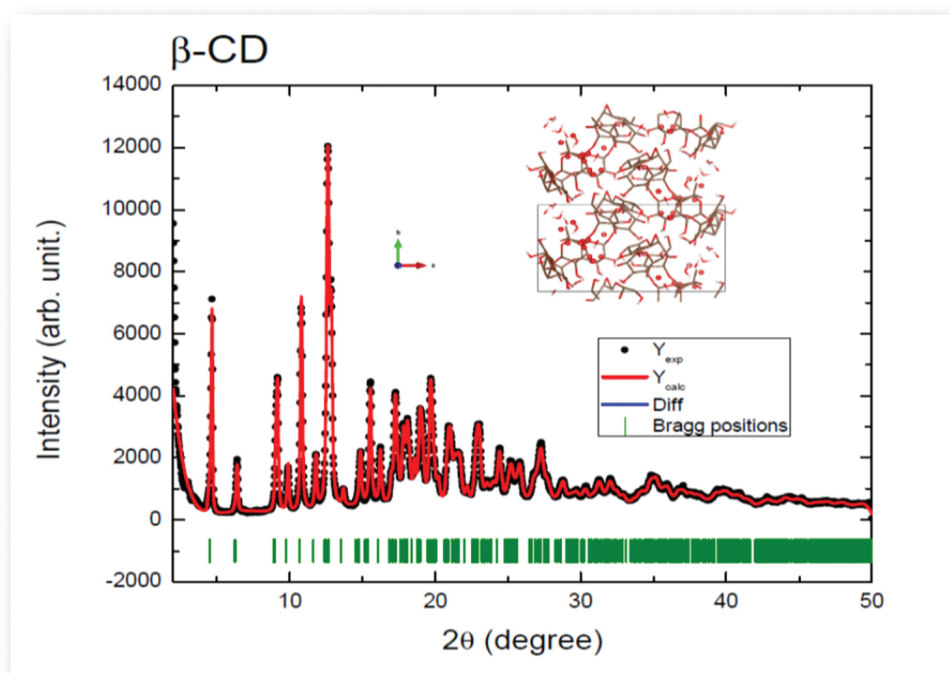


Figure 6. Diffractogram of crystalline β -cyclodextrin measured in a conventional diffractometer using Cu radiation. Also, Rietveld refinement was performed in order to obtain the crystal structure.

The time for collecting the data varies according to the application, for example, to study polymorphism in drugs. Good diffraction patterns of the crystalline material, using conventional X-ray instruments can be obtained in the range of 2–10 min per step. In configurations that use high efficiency X-ray sources (synchrotron) to samples mounted in a planar configuration, the collected time can be less than 1 min. The X-ray diffraction technique that is typically nondestructive (if the flux of X-ray is too high, we can observe the radiation damage effect that can affect the sample), needs 2–20 mg of sample, depending on the configuration geometry of the instrument and the application.

The quality of the sample and its correct preparation in order to perform the XRPD experiment influences significantly in the characterization or identification of the crystalline material. We can cite two factors related to the preparation of the sample that can affect the results:

1. Orientation of the crystallites: ideal sample has a big number of random oriented crystallites.
2. Statistics of particles orientation: the reproducibility of an X-ray pattern depends on the statistic of the particles orientation when the preferred orientation limits the degree in which the pattern represents the structure.

For these reasons, one must evaluate the statistics of the particle orientation and the degree of the preferred orientation before starting the identification and analysis.

The effect of the preferred orientation of the crystallites in a sample can be observed as the increase in the intensity on some of the peaks and the decrease in the intensity on others. The

variation of the intensity is proportional to the degree of preferred orientation. In some cases, the sample holder geometries of the diffractometer can also generate different set of relative intensities.

Using samples that show a relatively small number of crystallites results in a diffractogram with poor statistics. If the small population of the big crystallites does not represent all the possible orientations, the relative intensities will not be reproducible.

The effect of the preferred orientation on the particle orientation can be minimized by spinning the sample holder.

3.5. Amorphous materials

Amorphous materials (disorder, vitreous or amorphous materials) have characteristic diffractograms with large halos and do not show sharp peaks in the XRPD patterns. **Figure 7(c)** and **(d)** displays examples of a typical diffractogram of an amorphous material.

However, using suitable computational methods it is possible to extract structural information from this X-ray diffraction patterns. In this case, it is necessary a large angular range, typically from 1 to 100° in 2θ . Besides, the time to collect the data must be longer than the frequently

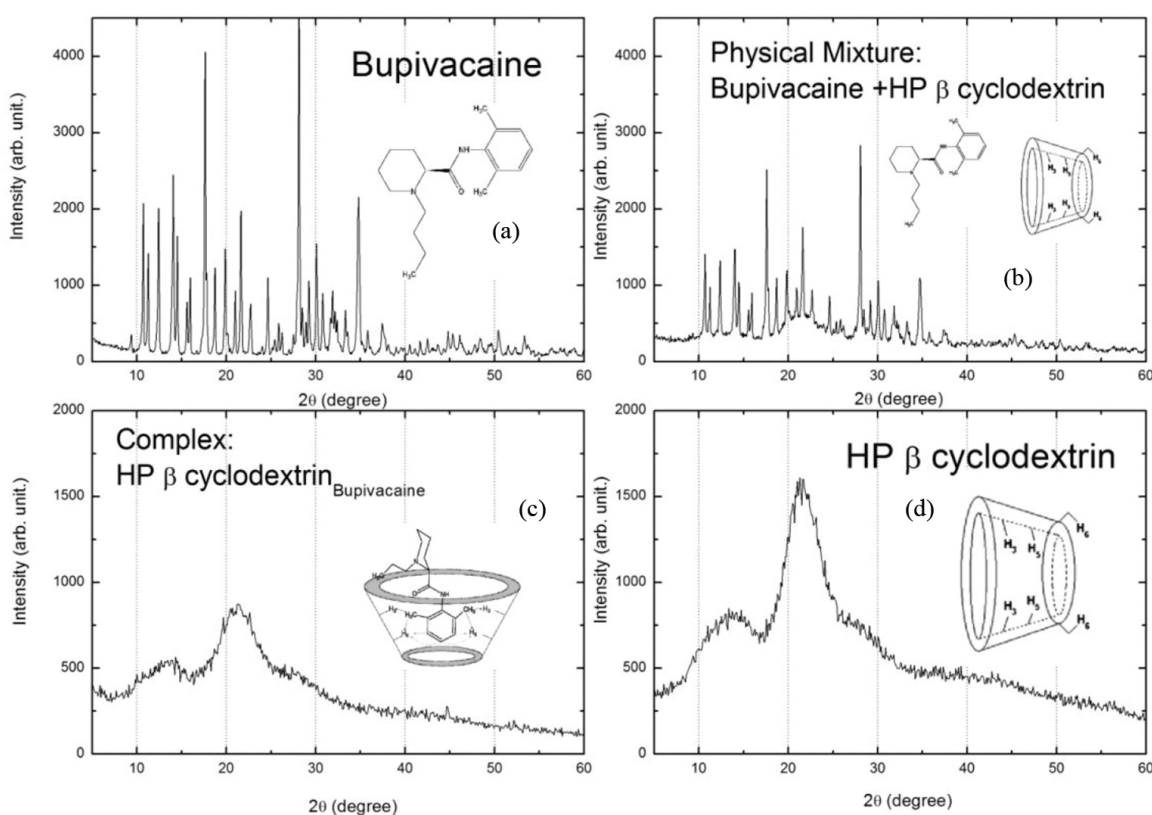


Figure 7. (a) Diffractogram of bupivacaine (BPV); (b) a physical mixture of BPV and HP- β -cyclodextrin; (c) complex of BPV and HP- β -cyclodextrin and (d) diffractogram of HP- β -cyclodextrin. Observe the amorphous diffractogram of the drug delivery systems, HP- β -cyclodextrin and the complex (drug delivery with drug).

used in conventional diffraction, due to the signal-noise ratio in an amorphous X-ray pattern be typically poor.

In order to obtain a good diffractogram through the X-ray diffraction technique for amorphous samples, usually one needs 5–100 mg of the samples, depending on the geometry of the instrument.

XRPD patterns, for crystalline materials or for amorphous materials, contain artifacts from the instrument, for example, background functions from the instrument, fingerprints from the sample holder, incoherent scattering (Compton), polarization and Lorenz effects, and air scattering. A relatively small pattern generated from the samples means that these artifacts represent a portion bigger of the overall diffracted intensity. Therefore, computational methods used to analyze amorphous materials are more sensitive to experimental artifacts.

3.6. Instrumentation

X-ray diffraction instrument used typically in conventional laboratories consists in three parts: (1) X-ray source; (2) sample holder, and (3) detector system.

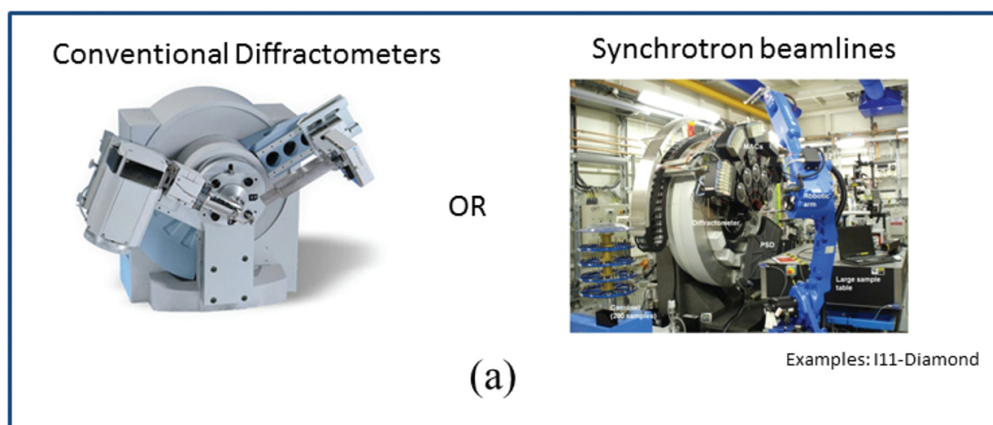
There are several X-ray sources that it can be possible to use in a conventional laboratory, but the most common is the copper source (Cu). Slits and optics are used to focus the X-ray incident beam in the sample and also, the X-ray diffracted waves scattered from the sample into the X-ray detector. In order to minimize artifacts from the sample (mentioned before), usually, the sample holder is spinning. The X-ray detectors can be punctual, linear or area. The detector area has the advantage of being fast in the data acquisition and also makes it possible to evaluate the statistics of the particle orientation and preferred orientation of the samples, through the analysis of the Debye rings in the detector.

Synchrotron sources can be used to measure special systems in order to collect high quality data.

Diffractometers can be operated typically in reflection (Bragg-Brentano) or transmission (Debye-Scherrer). In the reflection setup, the incident beam is reflected from the surface of the sample and the scattered beam is focused into the detector.

The X-ray penetrates several layers below the surface in organic samples. This means that the average diffracted surface is located below the surface of the sample. This penetration effect can yield to an error of a displacement of the peak positions in the diffraction pattern of the tenth of a degree

Errors caused by the displacement of the peaks happen due to the difficulty in the preparation of the sample in the sample holder (**Figure 8(b)**). The surface of the sample must be leveled with the surface of the flat sample holder (where the instrument is focused). Although computational methods can be used to correct the position of the peaks, the proper preparation of the sample is the only solution to solve this problem.

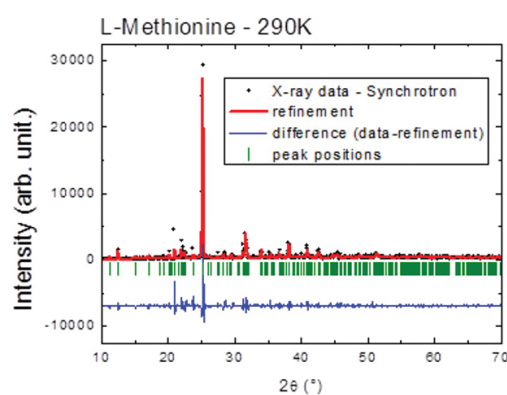


Sample preparation



(b)

Data Aquisition, Refinement, Structure



(c)

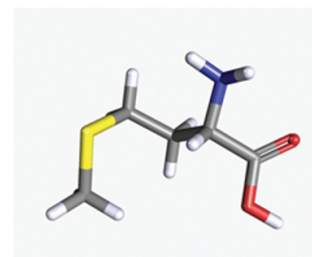


Figure 8. (a) Laboratory XRPD equipment or Synchrotron XRPD beamline can be used to characterize drug delivery systems and drugs; (b) preparation of samples; (c) some results from a biological material, L-methionine, measured at XRPD synchrotron beamline. Also observed the Rietveld refinement and the possible structure of the sample.

Usually measurement at low angles (below 2.5° in 2θ) is not appropriate due to the limitation of the instrument used mainly for big molecules, where it is expected to find reflections in the range from 0 to 2.5° . Measurements using the transmission setup can solve this limitation, when the instrument is properly set. In the transmission setup the X-ray incident beam pass through the sample. This configuration is possible for organic samples due to its relative transparency for X-rays. In this case, the sample does not need to be leveled with the sample holder surface, but the thickness of the sample is important and can cause errors in the displacement of the peaks. Besides, it is essential in this configuration that the sample holder is transparent to X-rays. In the case of amorphous materials, it is necessary an extra effort to operate the instrument in order to improve the quality of the data.

Acknowledgements

The authors acknowledge the financial support received by CNPq/Brazil and FAPESP (# grant 14/14457-5).

Author details

Margareth Kazuyo Kobayashi Dias Franco, Daniele Ribeiro de Araújo, Eneida de Paula, Leide Cavalcanti and Fabiano Yokaichiya

*Address all correspondence to: margareth_franco@yahoo.com.br; mkfranco@ipen.br

1 Brazilian Multipurpose Reactor, Nuclear and Energy Research Institute, IPEN, São Paulo, SP, Brazil

2 Human and Natural Sciences Center, Federal University of ABC, Santo André, SP, Brazil

3 Biochemistry and Tissue Biology Department, Biology Institute, State University of Campinas-Campinas, SP, Brazil

4 Chemical Engineering, State University of Campinas-Campinas, SP, Brazil

5 Department of Quantum Phenomena in Novel Materials, Helmholtz Zentrum Berlin, Berlin, Germany

References

- [1] Neubert. Potentials of new nanocarriers for dermal and transdermal drug delivery. *Eur. J. Pharm. Biopharm.* 2011;77(1–2).
- [2] Solarex. SX-40 & SX-50 Photovoltaic Modules [Internet]. http://www.trichord-inc.com/pricing/frames/content/solar_power.pdf. 1999
- [3] Mc Grath S, van Sinderen D (editors). (2007). *Bacteriophage: Genetics and Molecular Biology* (1st ed.). Caister Academic Press. <https://en.wikipedia.org/wiki/Bacteriophage>(ISBN 978-1-904455-14-1)
- [4] <http://www.virology.wisc.edu/virusworld/images/cpv-half-nuc.jpg>. 2014.
- [5] Grass RN, Robert N, Athanassiou EK, Stark WJ. Covalently functionalized cobalt nanoparticles as a platform for magnetic separations in organic synthesis". *Angew. Chem. Int. Ed.* 2007;46(26): 490912. doi:10.1002/anie.200700613. https://en.wikipedia.org/wiki/Magnetic_nanoparticles.
- [6] https://en.wikipedia.org/wiki/Nanoparticle#/media/File:Mesoporous_Silica_Nanoparticle.jpg. 2015.
- [7] <http://www.omicsonline.org/articles-images/2161-0398-2-105-g001.gif>.
- [8] <http://www.foresight.org/Conference/MNT7/Papers/Cagin3/>.

- [9] http://cmb.gu.se/english/research/organic-and-medicinal-chemistry/Biomedical_Photonics/projects/gold-nanoparticles-
- [10] <http://pubs.acs.org/doi/abs/10.1021/bm2010774>.
- [11] <http://image.slidesharecdn.com/lipoproteins-150424045513-conversion-gate02/95/lipoproteins-8-638.jpg?cb=1429869399>.
- [12] <http://www.pharmatutor.org/articles/nanocochleate-novel-bypass-of-conventional-drug-elivery-system>.
- [13] <http://www.ebioscience.com/media/images/resources/knowledge-center/product-line/efluor/efluor-nc/nc-technology/efluor-nanocrystal-compostion.png>.
- [14] <http://www.photonics.com/Article.aspx?AID=57396>.
- [15] <http://blogs.nottingham.ac.uk/malaysiaknowledgetransfer/files/2013/06/Siva001.jpg>.
- [16] <http://www.keystonenano.com/platform/liposomes>.
- [17] http://www.nature.com/nnano/journal/v3/n2/fig_tab/nnano.2008.13_F1.html.
- [18] <http://web.mit.edu/lms/www/images/Fig.%205B%20sm.jpg>.
- [19] <http://www.carbonallotropes.com/carbon-nanotubes/39-single-wall-carbon-nanotubes.html>.
- [20] http://www.nature.com/nnano/journal/v2/n4/fig_tab/nnano.2007.90_F1.html.
- [21] Oshiro A, da Silva DC, Santos ACM, Akkari ACS, de Araujo, Daniele R. Development of drug-delivery systems: strategies for new pharmaceutical formulations based on liposomal and micellar systems. *Supramolecular Chemistry, Nanotechnology* (1st ed.). São Paulo: Atheneu In: Alve WA. (Org.). 2014;vol.1; pp. 249–264.
- [22] Holowka E, Bhatia SK. *Drug Delivery, Material Design and Clinical Perspective*. Springer-Verlag New York. 2014. ISBN 978-1-4939-1998-7, DOI: 10.1007/978-1-4939-1998-7
- [23] Egelhaaf SU, Wehrli E, Muller M, Adrian M, Schurtenberger P. Determination of the size distribution of lecithin liposomes: A comparative study using freeze fracture, cryoelectron microscopy and dynamic light scattering. *J. Microsc (Oxf)*. 1996;184:214–228. (ISSN 0022-2720)
- [24] Evjen TJ, Hupfeld S, Barnert S, Fossheim S, Schubert R, Brandl M. Physicochemical characterization of liposomes after ultrasound exposure-mechanisms of drug release. *J. Pharm. Biomed. Anal*. 2013;78–79:118–122. DOI: 10.1016/j.jpba.2013.01.043
- [25] Zuidam NJ, de Vruh R, Crommelin Daan JA. (2003). *Characterization of Liposomes* In: *Liposomes: A Practical Approach*. Torchilin, Vladimir P, Weissig, Volkmar (eds). Oxford University Press, London (2nd ed.) pp. 31–78.
- [26] Glatter O, Kratky O. *Small Angle X-Ray Scattering*. Academic Press, London. 1982.

- [27] Glatter O. Scattering studies on colloids of biological interest (Amphiphilic Systems). *Progr. Colloid. Polym. Sci.* 1991;84:46–54.
- [28] Kratky O. The world of neglected dimensions, SAS of X-ray and neutrons of biological macromolecules. *Nova Acta Leopoldina NF* 55; 1983.
- [29] Trevisan J, Cavalcanti LP, Oliveira CLP, de la Torre L, Santana MH. Technological aspects and scalable enhanced processes for production of functional cationic liposomes as delivery system in gene therapy. In: *Non-viral Gene Therapy*. Yuan, X. (ed), Intech, Croatia OPEN ACCESS: <http://dx.doi.org/10.5772/17869>. (ISBN 978-953-307-538-9)
- [30] Oliveira CLP, Gerbelli BB, Silva ERT, Nallet F, Navailles L, Oliveira EA, Pedersen JS. Gaussian deconvolution: A useful method for a form-free modeling of scattering data from mono- and multilayered planar systems. *J. Appl. Crystallogr.* 2012;45:1278–1286.
- [31] <http://www.azom.com/equipment-details.aspx?EquipID=3095>. 2016.
- [32] Brzustowicz MR, et al. X-ray scattering from unilamellar lipid vesicles. *J. Appl. Cryst.* 2005;15:38:126–131.
- [33] Gasperini A, Puentes-Martinez X, Balbino T, Rigoletto T, Corrêa G, Cassago A, Portugal R, de La Torre LG, Cavalcanti LP. Association between cationic liposomes and low molecular weight hyaluronic acid. *Langmuir* (2015) 31:3308.
- [34] Balbino TA, Gasperini AAM, Oliveira CLP, Azzoni A, Cavalcanti LP, de la Torre L. Correlation of the physico-chemical and structural properties of pDNA/cationic liposome complexes with their in vitro transfection. *Langmuir*. 2012;28:11535.
- [35] Castelletto V, Parras P, Hamley IW, Bäverböck P, Pedersen JS, Panine P. Wormlike micelle formation and flow alignment of a Pluronic block copolymer in aqueous solution. *Langmuir*. 2007;23(13):6896–6902.
- [36] Artzner F, Geiger S, Olivier A, Allais C, Finet S, Agnely F. Interactions between poloxamers in aqueous solutions: Micellization and gelation studied by differential scanning calorimetry, small angle X-ray scattering, and rheology. *Langmuir*. 2007;23(9):5085–5092.
- [37] Alexandridis P, Hatton T. Poly(ethylene oxide)-poly(propylene oxide)-poly(ethylene oxide) block copolymer surfactants in aqueous solutions and at interfaces: Thermodynamics, structure, dynamics, and modeling. *Coll. Surf. A: Physicochem. Eng. Asp.* 1995;96:1–46.
- [38] Santos Akkari AC, Ramos Campos EV, Keppler AF, Fraceto LF, de Paula E, Tófoli GR, de Araujo DR. Budesonide-hydroxypropyl- β -cyclodextrin inclusion complex in binary poloxamer 407/403 system for ulcerative colitis treatment: A physico-chemical study from micelles to hydrogels. *Colloids. Surf. B: Biointerfaces*. 2016;38:138–147.
- [39] Oshiro A, da Silva DC, de Mello JC, de Moraes VW, Cavalcanti LP, Franco MK, Alkschbirs MI, Fraceto LF, Yokaichiya F, Rodrigues T, de AraujoDR. *Pluronics f-127/l-*

81 binary hydrogels as drug-delivery systems: Influence of physicochemical aspects on release kinetics and cytotoxicity. *Langmuir*. 2014;30(45):13689–13698.

- [40] Mello JC, Moraes VW, Watashi CM, da Silva DC, Cavalcanti LP, Franco MK, Yokaichiya F, de Araujo DR, Rodrigues T. Enhancement of chlorpromazine antitumor activity by Pluronic F127/L81 nanostructured system against human multidrug resistant leukemia. *Pharmacol. Res.* 2016;111:102–112.
- [41] Avachat AM, Parpani SS. Formulation and development of bicontinuous nanostructured liquid crystalline particles of efavirenz. *Colloids. Surf. B: Biointerfaces*. 2015;126:87–97.
- [42] Chen Z, Liu Z, Qian F. Crystallization of bifonazole and acetaminophen within the matrix of semicrystalline, PEO-PPO-PEO triblock copolymers. *Mol. Pharm.* 2015;12(2): 590–599.
- [43] Kopeček J, Yang J. Smart self-assembled hybrid hydrogel biomaterials. *Angew. Chem. Int. Ed. Engl.* 2012;51:7396–7417.
- [44] Zhang L, Zhang N. How nanotechnology can enhance docetaxel therapy. *Int. J. Nanomed.* 2013;8:2927–2941.
- [45] Ricardo NM, Ricardo NM, Costa Fde M, Bezerra FW, Chaibundit C, Hermida-Merino D, Greenland BW, Burattini S, Hamley IW, Nixon KS, Yeates SG. Effect of water-soluble polymers, polyethylene glycol and poly(vinylpyrrolidone), on the gelation of aqueous micellar solutions of Pluronic copolymer F127. *J. Colloid. Interface. Sci.* 2012;368(1):336–341.
- [46] Nambam JS, Philip J. Thermogelling properties of triblock copolymers in the presence of hydrophilic Fe_3O_4 nanoparticles and surfactants. *Langmuir*. 2012;28(33):12044–12053.
- [47] Kerkhofs S, Willhammar T, Van Den Noortgate H, Kirschhock CE, Breynaert E, Van Tendeloo G, Bals S, Martens JA. Self-assembly of Pluronic F127-silica spherical core-shell nanoparticles in cubic close-packed structures. *Chem. Mater.* 2015;27(15):5161–5169.
- [48] Simões SM, Veiga F, Torres-Labandeira JJ, Ribeiro AC, Sandez-Macho MI, Concheiro A, Alvarez-Lorenzo C. Syringeable Pluronic- α -cyclodextrin supramolecular gels for sustained delivery of vancomycin. *Eur. J. Pharm. Biopharm.* 2012;80(1):103–112.
- [49] Pradal C, Jack KS, Grøndahl L, Cooper-White JJ. Gelation kinetics and viscoelastic properties of Pluronic and α -cyclodextrin-based pseudopolyrotaxane hydrogels. *Biomacromolecules*. 2013;14(10):3780–3792.
- [50] Shih KC, Li CY, Li WH, Lai HM. Fine structures of self-assembled beta-cyclodextrin/Pluronic in dilute and dense systems: A small angle X-ray scattering study. *Soft. Matter*. 2014;10(38):7606–7614.

- [51] Wunderlich B. A classification of molecules and transitions as recognized by thermal analysis. *Thermochim. Acta.* 1999;340/41:37–52.
- [52] Als-Nielsen J, McMorrow D. *Elements of Modern X-ray Physics.* Wiley, New York ; Chichester. 2001; xi:318 p.
- [53] Cullity BD, Stock SR. *Elements of X-ray Diffraction.* Addison-Wesley Reading, MA. 1978
- [54] Klug HP, Alexander LE. *X-ray Diffraction Procedures for Polycrystalline and Amorphous Materials.* Wiley, New York; 2nd ed, 1974; xxv:966 p.
- [55] Warren BE. *X-ray Diffraction.* Dover Publications, New York, 1990; vii:381p.
- [56] Young RA, *The Rietveld Method* (International Union of Crystallography Oxford University Press, [Chester, England] Oxford; New York, 1993; x: 298 p.
- [57] Zachariasen WH, *Theory of X-ray Diffraction in Crystals* (J. Wiley and Sons, Inc. Chapman and Hall, Ltd, New York London, 1945;vi: 1 l 255 p.